

No Universality for Electron’s Power-Law Index (p) in Gamma-Ray Bursts and Other Relativistic Sources

Rongfeng Shen [★], Pawan Kumar, and Edward L. Robinson

Department of Astronomy, University of Texas at Austin, 1 University Station C1400, Austin, TX 78712, USA

ABSTRACT

The Gamma-Ray Burst (GRB) prompt emission is believed to be from highly relativistic electrons accelerated in relativistic shocks. From the GRB high-energy power-law spectral indices β observed by the Burst and Transient Source Experiment (BATSE) Large Area Detectors (LAD), we determine the spectral index, p , of the electrons’ energy distribution. Both the theoretical calculations and numerical simulations of the particle acceleration in relativistic shocks show that p has a universal value $\approx 2.2 – 2.3$. We show that the observed distribution of p during GRBs is not consistent with a δ -function distribution or an universal p value, with the width of the distribution ≥ 0.54 . The distributions of p during X-ray afterglows are also investigated and found to be inconsistent with a δ -function distribution. The p -distributions in blazars and pulsar wind nebulae are also broad, inconsistent with a δ -function distribution.

Key words: gamma rays: bursts – gamma rays: relativistic shocks – statistical analysis

[★] E-mail: rfshen@astro.as.utexas.edu.

1 INTRODUCTION

GRBs are observed to have non-thermal spectra during its prompt emission phase (Band et al. 1993). It is widely believed that the synchrotron radiation and/or the inverse Compton scattering are the likely emission mechanism(s) for GRB's prompt hard X-ray and γ ray emission. The electrons accounting for these emissions are thought to be accelerated in relativistic shocks in GRBs. According to the shock diffusive acceleration model, particles are accelerated when they repeatedly cross a shock front, and the competition between the particle's energy gain and escape probability per shock crossing cycle leads to a power-law spectrum for the particles:

$$N(\gamma)d\gamma \propto \gamma^{-p}d\gamma, \quad (1)$$

where γ is the Lorentz factor of the particle (e.g., Blandford & Ostriker 1978). For non-relativistic shocks, the value of p depends on the the compression ratio of the flow stream across the shock; while in relativistic or ultra-relativistic shocks, which is most likely the case in GRBs, analytical and numerical studies show that p has an “universal” value, $\approx 2.2 - 2.3$ (Kirk et al. 2000, Achterberg et al. 2001, Bednarz & Ostrowski 1998, Lemonine & Pelletier 2003).

The work reported in this paper is to investigate the “universality” of the power-law index p for GRBs, which we calculate directly from the high-energy (0.1 – 2 MeV) photon spectrum of GRBs (Preece et al. 1998, 2000), assuming the spectrum is from synchrotron or synchrotron self-inverse-Compton emission of the power-law distributed highly relativistic electrons, using the relations between p and the spectral index, β , of the high-energy power-law photon spectrum.

In §2, we describe the GRB spectral data set used and the process of determining the parent p -distribution. In §3, we examine the contributions from the spectral fit procedure and the time averaging effect to the dispersion of the parent distribution of p . The p -distributions derived from BeppoSAX GRBs and from HETE-2 GRBs, X-ray flashes and X-ray rich GRBs

are presented in §4. We determine the p -distributions for X-ray afterglows in §5 and for blazars and pulsar wind nebulae in §6. A summary and discussions are given in §7.

2 THE DISTRIBUTION OF P IN GRBS

2.1 The GRB spectral sample

For our analysis, we use the BATSE GRB Spectral Catalog presented by Preece et al. (2000). In the catalog, the time sequences of spectral fit parameters for 156 bright bursts are presented, using mostly the high energy and time resolution data from the Large Area Detectors (LAD), which covers an energy range of typically 28 - 1800 keV. All bursts have at least 8 spectra in excess of 45σ above background. The spectral models used in fit are (i) 'Band' function; (ii) Comptonized spectral model (a power-law with an exponential cut-off); (iii) Broken Power-Law model; and (iv) Smoothly Broken Power-Law model. The 'Band' function, the one used most frequently, is an empirical function (Band et al. 1993)

$$N(E) = A \begin{cases} (E/100)^\alpha \exp[-E(2+\alpha)/E_{peak}], & E < \frac{\alpha-\beta}{2+\alpha} E_{peak} \\ \left[\frac{(\alpha-\beta)E_{peak}}{100(2+\alpha)} \right]^{\alpha-\beta} \exp(\beta-\alpha)(E/100)^\beta, & E \geq \frac{\alpha-\beta}{2+\alpha} E_{peak} \end{cases}$$

where $N(E)$ is the photon counts, A is the amplitude, α is the low-energy spectral index, β the high-energy spectral index, and E_{peak} is the peak energy in the νF_ν spectrum (when $\beta < -2$).

Since we are here caring about the high-energy power-law portion of the GRB spectra, and also because one possible source of systematic error in the spectral parameter determination arises in selecting different spectral models for different bursts (Preece et al. 2002), only the spectral parameters of those 'Band' function fitted spectra are selected for our analysis.

One of our major concerns is to select the sample of spectra for which β is reliably determined. The BATSE burst signal-to-noise ratio decreases at higher energies as a result of fewer photon flux and the decreased detector efficiency. In particular, β may not be well

determined if E_{peak} is close to the higher limit of the LAD energy range, E_{max} (≈ 2 MeV) (Preece et al. 1998), thus we must choose those spectra with E_{peak} much lower than E_{max} . Therefore, we select the spectrum for which 100 keV $< E_{peak} < 200$ keV and the error in β is less than $0.1 |\beta|$. This gives a total sample of 395 spectra for 78 bursts.

2.2 Distribution of p and its narrowing

For electrons' distribution given by a power-law:

$$N(\gamma_e) \propto \gamma_e^{-p}, \text{ for } \gamma_e > \gamma_{min}, \quad (2)$$

the emergent high energy synchrotron spectrum is asymptotically a power law function: $F_\nu \propto \nu^{-(p-1)/2}$ for $\nu_m < \nu < \nu_c$ (“slow cooling” regime) and $\propto \nu^{-p/2}$ for $\nu > \nu_c$ (“fast cooling” regime), where $\nu_m = \nu_{syn}(\gamma_{min})$ is the synchrotron injection frequency, and $\nu_c = \nu_{syn}(\gamma_c)$ is the synchrotron cooling frequency above which the synchrotron energy loss becomes important.

The spectral index, p , of shock accelerated electrons is associated with the high-energy power-law photon index, β , of GRB photon spectrum, by either $\beta = -p/2 - 1$ (“fast cooling” regime) or $\beta = -(p+1)/2$ (“slow cooling” regime) depending on relative positions of ν_m and ν_c and on which portion of the spectrum is detected. There is one regime, $\nu_c < \nu < \nu_m$, in which $\beta = -3/2$, independent on p . This case can be ruled out by discarding those spectra with $\beta \geq -3/2$ from our sample. We found only one with $\beta \geq -3/2$ in the BATSE sample of 395 spectra and discarded it.

Piran (2004) argues that the fast cooling must take place during the GRB prompt phase and the reasons are: (i) the relativistic shocks must radiate their energy efficiently, to avoid a serious inefficiency problem; (ii) the electrons must cool rapidly in order that the fast variability could be observed. But there is no firm evidence to date that could rule out the slow cooling case for the GRB itself, since it is difficult to measure the values of γ_c and γ_{min} for a specific burst. Thus in our analysis, we assume that each GRB spectrum above

E_{peak} could be in either slow cooling or fast cooling regime, so as to minimize the width of p distribution.

First we plot distribution of p by assuming all spectra are in fast cooling regime. Then we make the distribution narrower by relaxing this constraint. Basically the narrowing process is to move some left-hand part of the distribution to the right by adding 1 to p and assuming this part of sample are in slow cooling regime, since there is a difference of 1 about p value between the two regimes. The algorithm used is described below.

Several algorithms are implemented to get the narrowest distribution. In the most straightforward one, each spectra has the freedom of calculating p from β either in “fast cooling” or “slow cooling” regime, so the number of possible distributions is 2^N for a sample of N spectra. The distribution having the smallest standard deviation is chosen as the narrowest one. This algorithm works well only for $N < 20$ because of the computer program’ running time. For $N > 20$, we divide the overall range of the sample’s β distribution into 20 equal-width bins and treat the spectra with β ’s located in each bin indistinguishably. Then we apply the first algorithm to the 20 bins. In an alternative algorithm, we start with the histogram of p calculated in the “fast cooling” regime and mark a demarcation line within and close to the lower limit of the range of p . Then all p ’s at left to the line in the histogram are moved to right by adding 1 to p , and the new histogram’s standard deviation is calculated. Repeat it after shifting the demarcation line rightward by a step of 0.01 on the p -axis. Finally the smallest standard deviation, hence the narrowest distribution, is found. It turns out that both algorithms give the same results for most of the samples presented in this paper. For one sample where minor difference exists between two algorithms’ results, we use the narrower one.

We show the results of the analysis for BATSE bursts in Figure 1. Note that all the errors presented in this paper are at 1σ level. The parent distribution of p for BATSE bursts has a width of 0.54 at a 14σ confidence level. The method that estimates the mean and the width of the parent distribution of p is described below. Note that the mean value of p is

≈ 3 , substantially larger than that for the distribution before the minimization, which is an artifact of choosing some of the spectra to be in the “slow cooling” regime, equivalent to moving the left part of the histograms in the upper panels rightward, in order to minimize the width of the distribution.

2.3 Statistical description of the narrowness of p ’s distribution

The observed distribution of p plotted in Fig. 1 is a convolution of the measurement error distribution and the true distribution (or parent distribution) of p ’s. What we want to know is the true distribution p . We use the maximum likelihood method to estimate the true p -distribution. Let us say the true distribution of p is Gaussian,

$$P(p) = \frac{1}{\sqrt{2\pi}\sigma_p} \exp\left[-\frac{1}{2}\frac{(p - \bar{p})^2}{\sigma_p^2}\right]. \quad (3)$$

Further, we assume the measurement errors have Gaussian distributions too. Then the probability distribution for any one measurement (p_i, σ_i) is the convolution of two Gaussians, which is the Gaussian

$$P(p_i, \sigma_i, \bar{p}, \sigma_p) = \frac{1}{\sqrt{2\pi}(\sigma_p^2 + \sigma_i^2)^{1/2}} \exp\left[-\frac{1}{2}\frac{(p_i - \bar{p})^2}{\sigma_p^2 + \sigma_i^2}\right]. \quad (4)$$

The likelihood function for the set of n measurements p_i, σ_i is

$$L = \prod_{i=1}^n \frac{1}{\sqrt{2\pi}(\sigma_p^2 + \sigma_i^2)^{1/2}} \exp\left[-\frac{1}{2}\frac{(p_i - \bar{p})^2}{\sigma_p^2 + \sigma_i^2}\right]. \quad (5)$$

The principle of the Maximum Likelihood Estimate is that, the best estimates of \bar{p} and σ_p^2 are the ones that maximize L . Take

$$l = \ln L = -\frac{1}{2} \sum_i^n \frac{(p_i - \bar{p})^2}{\sigma_p^2 + \sigma_i^2} - \frac{1}{2} \sum_i^n \ln(\sigma_p^2 + \sigma_i^2), \quad (6)$$

then the maximum occurs when the following equations

$$\frac{\partial l}{\partial \bar{p}} \bigg|_{\hat{p}, \hat{\sigma}_p^2} = 0, \quad (7)$$

$$\frac{\partial l}{\partial (\sigma_p^2)} \bigg|_{\hat{p}, \hat{\sigma}_p^2} = 0 \quad (8)$$

have their solution at $\bar{p} = \hat{p}$ and $\sigma_p^2 = \hat{\sigma}_p^2$, where “ $\hat{\cdot}$ ” symbolizes the best estimation of the parameters. If we assume that the distribution of \hat{p} and $\hat{\sigma}_p^2$ are both Gaussian, then one can show that the variances of \hat{p} and $\hat{\sigma}_p^2$ are

$$\sigma_{\hat{p}}^2 = - \left[\frac{\partial^2 l}{\partial \bar{p}^2} \Big|_{\hat{p}, \hat{\sigma}_p^2} \right]^{-1}, \quad (9)$$

$$\sigma_{\hat{\sigma}_p^2}^2 = - \left[\frac{\partial^2 l}{\partial (\hat{\sigma}_p^2)^2} \Big|_{\hat{p}, \hat{\sigma}_p^2} \right]^{-1}, \quad (10)$$

respectively. So the best estimate of the parameters of true distribution of p are obtained by numerically solving equations (7) and (8), and their associated errors are calculated through equations (9) and (10).

3 SYSTEMATIC ERRORS IN β

3.1 The ‘Band’ function fit to the spectra

Preece et al. (2000) carried out a Band function fit to GRB spectra observed by BATSE, and this way determine the high energy power-law index (β) and the random error in β due to error in the observed spectral energy distribution. There is also a systematic error in β resulting from the finite bandwidth of the BATSE detector, which was not reported in Preece et al., and we estimate it here. The purpose of this exercise is to estimate the contribution of this systematic error, and its dependence on the peak of the spectrum (E_{peak}), to the dispersion in the p -distribution.

The systematic error arises because the synchrotron spectrum does not make a sharp transition from one power-law index to another when one crosses a characteristic frequency. In particular, the steepening of the spectrum to $\nu^{-p/2}$ above the synchrotron and cooling frequencies does not occur suddenly at E_{peak} , but instead the spectrum approaches this theoretical value asymptotically at $E \gg E_{peak}$.

Since the spectrum is observed in a finite energy range, the measured spectral index will always be somewhat smaller than the true asymptotic value by an amount that depends on

the ratio of E_{max} and E_{peak} (E_{max} is the highest energy photon that the detector is sensitive to). The larger the E_{max}/E_{peak} is the smaller the systematic error in β would be, and this dependence on E_{peak} causes some broadening of the observed β distribution.

To estimate this systematic error we generate synthetic spectra with different values for E_{peak} , and carry out a Band function fit to the synthetic spectra to determine β and its deviation from the true asymptotic value.

The synthetic synchrotron spectra is calculated for a relativistic homogeneous shell. The electron distribution function behind the shock is taken to be a single power-law function: $N(\gamma_e) \propto \gamma_e^{-p}$, for $\gamma > \gamma_{min}$, where $m_e c^2 \gamma_{min}$ is the minimum electron energy after they cross the shock front. The magnetic field in the shell is taken to be uniform and the energy density is the field is some fraction (ϵ_B) of the thermal energy density of the shocked fluid; γ_{min} and ϵ_B are chosen so that the peak of the spectrum, E_{peak} , is at some desired value. As electrons move down-stream from the shock front they cool via the synchrotron and inverse-Compton processes, and their distribution function is modified. We calculate the effect of this cooling on electron distribution functions using a self consistent scheme described in Panaiteescu & Mészáros (2000) and McMahon et al. (2006).

The synchrotron spectrum, for a given electron distribution, in the shell comoving frame is calculated as described in detail by Sari et al. (1998) (also see section 2.2). The spectrum in the observer frame is calculated by integrating the spectral emissivity in the comoving frame over the equal-arrival-time surface as described in Kumar & Panaiteescu (2000). Errors are then added to this spectrum in a way that mimics the real GRB spectrum.

The synthetic spectrum for a known p is fitted to the Band function in a finite energy range corresponding to the BATSE energy coverage. By varying E_{peak} of the generated spectra we determine the discrepancy between fitted value and “true” value of β as a function of E_{max}/E_{peak} . The results are shown in Figure 2. We find the fit always gives a smaller β (in absolute value) than the true asymptotic value and that the “observed” β does indeed depend on E_{max} . The error in β is about 10% when E_{max}/E_{peak} is order unity, whereas

the error is $\sim 5\%$ when $E_{max}/E_{peak} \sim 20$. The error also depends on the p value as shown in Figure 2; for E_{peak} located between 100 keV to 200 keV, $E_{max} = 1.8$ MeV, and $p = 2.5$, the contribution of this systematic error to the dispersion in β is less than 1.3% – the corresponding contribution to the dispersion in p is $\sigma_p < 0.03$.

We have also carried out a similar calculation for the synchrotron self- inverse-Compton (SSC) spectrum for a population of synchrotron electrons. The incident photons are the synchrotron photons due to the same population of electrons that contribute to inverse-Compton scatterings. The synchrotron radiation is taken to be homogeneous and isotropic in the shell comoving frame, and its spectrum is calculated as described above. The overall SSC spectrum is obtained by the convolution of the synchrotron spectrum and electron energy distribution using equation (7.28 a) in Rybicki & Lightman (1979). The curvature in the SSC spectrum is due to the convolution of the incident spectrum and the electron distribution, and we find that the asymptotic value for the SSC power-law index is reached when $E_{max}/E_{peak} \sim 100$. For this reason we find that for the SSC case, the systematic error in β is $\sim 13\%$ for the typical E_{max}/E_{peak} in BATSE bursts. The dispersion in p caused by E_{peak} being distributed between $E_{peak} = 100$ keV to $E_{peak} = 200$ keV is, however, small – $\sigma_p < 0.04$.

These results show that the discrepancy between the fitted value and the “true” value of β is small and dependent on E_{max}/E_{peak} , but its dependence on E_{max}/E_{peak} is too small to account for the observed dispersion in the p distribution.

3.2 Time-averaging effect

Another source of systematic error in β is the time-averaging of multiple spectra undergoing spectral evolution, i. e., E_{peak} evolving with flux (Ford et al. 1995, Crider et al. 1999). The flux-weighted time-averaging of multiple ‘Band’ spectra may distort the intrinsic high-energy power law.

To examine this effect, we select BATSE time-resolved spectra with E_{peak} in 100 - 200

keV and in 200 - 300 keV, respectively, divide them into non-evolving groups and evolving groups, and analyze their p distributions separately. The results are shown in Table 1. We find the evolving spectra groups tend to have flatter p or β , which may be an outcome the time-averaging effect. But the widths of p distributions for two groups are consistent with each other, showing that the time-averaging does not contribute to observed dispersion in p in Figure 1.

The time-averaging effect is further examined when we use an early BATSE spectral catalog by Band et al. (1993) in which the time-integrated spectrum of each burst is fitted with the ‘Band’ function. We restrict our samples to those with $E_{peak} \leq 300$ keV, and error in β less than $0.1 |\beta|$, which gives a sample of 32 spectra from the catalog of 54 GRBs. The p distribution is shown in Figure 3. Comparing with Figure 1, one can see that it has approximately the same σ_p as that for the time-resolved GRB spectra. This supports that the time-averaging effect has no impact on the observed dispersion in p .

4 ***P*-DISTRIBUTIONS FOR BEPPOSAX GRBS AND HETE-2 XRFS, XRRS AND GRBS**

We also analyzed a sample of 11 GRBs observed by BeppoSAX. The combined (2 - 700 keV) Wide Field Cameras (WFC) and Gamma-Ray Burst Monitor (GRBM) spectra for these bursts are fitted with the ‘Band’ function by Amati et al. (2002). The narrowest distribution of p for this sample is shown in Figure 4 left panel. It has the same estimated mean value of p as in the BATSE bursts, and the width of the parent distribution for p is consistent with that for the BATSE bursts. The larger errors in $\langle p \rangle$ and σ_p are due to the smaller size of the BeppoSAX sample.

Sakamoto et al. (2005) present a catalog of X-ray flashes (XRFs), X-ray-rich (XRR) GRBs and GRBs observed by HETE-2 WXM (2 - 25 keV) and FREGATE (7- 400 kev) instruments. Among 45 bursts in the catalog, 16 bursts have measured high-energy power-law photon index, β , which is obtained through the spectral fit with the ‘Band’ function or

a single power-law model. For those XRF spectra fitted by a single power law, it is found that $\beta < -2$. Sakamoto et al. (2005) explain this as that we are observing the high-energy power-law portion of their “Band”-function spectra. Two GRBs (GRB 020813 and 030519) for which “Band” model is used have E_{peak} lying near or above the upper limit of FREGATE energy range, so we exclude them here. We also exclude XRF 030528 which has a large error in β . The final HETE-2 sample we considered comprises 7 XRFs, 4 XRRs and 2 GRBs. The p distribution is shown in Figure 4 right panel.

5 P-DISTRIBUTION FOR X-RAY AFTERGLOWS

We also determine the distribution of p during the X-ray afterglows. We use a catalog of X-ray afterglows observed by BeppoSAX compiled by De Pasquale et al. (2005) and a catalog of X-ray afterglows observed by Swift (O’Brien et al. 2006). In De Pasquale et al. (2005)’s catalog, 15 X-ray afterglow spectra are fitted with a Galactic-and-extragalactic absorbed single power law. We use 14 out of them for our analysis and exclude GRB 000210 which has an extremely large error in measured β . In O’Brien et al. (2006)’s Swift catalog of 40 X-ray afterglows, we select samples with small errors, $\sigma(\beta_i) < 0.1|\beta_i|$, and discard a sample with extremely large $|\beta|$ ($= 5.5$). We also discard 4 samples with $\beta_i \geq -3/2$ because these β values indicate the X-ray band probably lies between ν_c and ν_m ($\nu_c < \nu_X < \nu_m$), where the asymptotic spectral index is $\beta = -3/2$ and carries no information about p . This gives 28 samples from the catalog.

The p -distributions for the two afterglow samples are shown in Figure 5. For the BeppoSAX afterglows, the narrowest distribution is consistent with a δ -function distribution within 1σ errors; for the Swift afterglows, it is not. The smaller estimated width of the parent p -distribution for BeppoSAX afterglows, we suspect, is due to larger errors in photon indices β_i of the BeppoSAX sample, $\langle \sigma_i(\beta) \rangle = 0.26$, than the Swift sample which has $\langle \sigma_i(\beta) \rangle = 0.10$.

6 DISTRIBUTION OF P IN BLAZARS AND PULSAR WIND NEBULAE

6.1 Blazars

Blazars are active galactic nuclei with the relativistic jet pointed toward us. The nonthermal spectra of blazars are due to synchrotron or/and inverse Compton emission of relativistic electrons accelerated by shocks within the jet (Blandford & Königl 1979, Sikora et al. 1994).

Donato et al. (2005) present a spectral catalog of BeppoSAX six years of observations of Blazars at 0.1 - 50 keV. This catalog comprises three classes of blazars, namely low-luminosity sources (High-energy peaked BL Lacs, or HBLs), mid-luminosity sources (Low-energy peaked BL Lacs, or LBLs) and high-luminosity sources (Flat Spectrum Radio Quasars, or FSRQs). The three classes have different locations of synchrotron peak. X-rays from HBLs are likely to be above the peak of synchrotron spectrum, thus have steep X-ray spectra ($\beta < -2$), while FSRQs and LBLs in X-ray band have more contribution from inverse Compton component and thus have flatter spectra.

From this catalog we use 44 spectra of 33 HBLs (some sources have multi-epoch spectra) that are best fitted by single power-laws. The errors of fitted photon indices reported in Donato et al. (2005) are at 90% confidence level which we convert to $1-\sigma$ errors. The distribution of p derived from their photon spectral indices is shown in Figure 6. We find that the distribution of p for blazars is not consistent with a δ -function distribution: $\sigma_p = 0.22 \pm 0.03$ after the narrowing.

6.2 Pulsar wind nebulae

Power-law nonthermal spectra are also often observed in pulsar wind nebulae (PWNe) of rotation-powered pulsars. The nebular emission is the synchrotron radiation from charged particles heated by the termination shock in relativistic outflow (winds) from the pulsar (see Arons (2002) for a review). Gotthelf (2003) presents a catalog of nine bright Crab-like pulsar systems with Chandra observations and the photon indices of pulsar nebulae, β_{PWN} , and their 90% confidence errors are provided. We derive the distribution of p from β_{PWN}

with the β_{PWN} errors converted into 1σ errors and find that $\sigma_p = 0.59 \pm 0.15$, $\langle p \rangle = 1.72 \pm 0.20$ assuming the X-ray band is in the fast cooling regime. After narrowing, the narrowest distribution has $\sigma_p = 0.24 \pm 0.07$, $\langle p \rangle = 2.04 \pm 0.09$.

7 SUMMARY AND DISCUSSIONS

Motivated by theoretical calculations and numerical simulations showing that the shock-accelerated electrons in relativistic shocks have a power-law distribution with an universal index $p \simeq 2.2 - 2.3$, we have determined the values of p from γ -ray and X-ray spectra for a number of relativistic sources such as GRBs (prompt emissions and afterglows), blazars and pulsar wind nebulae.

The maximum likelihood estimate of the width of the parent distribution for GRB prompt emission is found to be quite broad, $\sigma_p = 0.51 \pm 0.02$; the probability that the distribution is consistent with a δ -function is extremely small, and therefore this result does not support that there is an universal p .

We have considered the systematic errors in photon index due to spectra fit and time averaging of spectra and their contributions to the scatter in p distribution. We have shown that those contributions are very small for GRBs and can not explain the scatter in p distribution.

For X-ray afterglows of GRBs, the p -distribution of the BeppoSAX sample can not rule out a possibility that the parent distribution is a δ -function distribution; however, a larger sample of Swift afterglows is inconsistent with a δ -function parent distribution. We point out that the smaller width of parent distribution for the BeppoSAX sample is due to its larger measurement error in β .

Analysis of 44 blazar spectra and 9 pulsar wind nebulae shows that the distributions of p for blazars and pulsar wind nebulae (PWNe) are also broad, not consistent with a δ -function distribution.

Possible situations in which the “universality” of p could break are: (i) The shock is Mildly

relativistic (cf. Kirk et al. 2000); (ii) The magnetic field is oblique to the shock normal (Baring 2005); (iii) The nature and strength of the downstream magnetic turbulence are varying (Ostrowski & Bednarz 2002, Niemiec & Ostrowski 2004). A non-Fermi acceleration in a collisionless plasma shock was studied by Hededal et al. (2004), in which electrons are accelerated and decelerated instantaneously and locally, by the electric and magnetic fields of the current channels formed through the Weibel two-stream instability. It is not known whether an “universality” of p could hold for this mechanism. The “universality” of p might not happen in non-shock accelerations; for instance, in an alternative model for GRBs (Lyutikov & Blandford 2003), the energy is carried outward via magnetic field or Poynting flux. The particles accounting for the γ -ray emissions are accelerated by magnetic field reconnection which may also produce a power-law spectra of accelerated particles with a variable p (however, this is still poorly understood).

ACKNOWLEDGMENTS

This work was supported in part by a NSF (AST-0406878) grant and a NASA-Swift-GI grant. RFS thank Dr. Volker Bromm for his suggestion which helps improve this work.

REFERENCES

Achterberg, A., Gallant, Y. A., Kirk, J. C., Guthmann, A. W., 2001, MNRAS, 328, 393
 Amati, A., Frontera, F., Tavani, M., et al., 2002, A&A, 390, 81
 Arons, J., 2002, in ASP Conf. Ser. 271, Neutron Stars in Supernova Remnants, ed. P. O. Slane & B. M. Gaensler, San Francisco: ASP, p.71 (astro-ph/0201439)
 Band D., Matteson J., Ford L. et al. 1993, ApJ, 413, 281
 Baring M. G., 2005, astro-ph/0502156, Advances in Space Research, in press
 Bednarz, J., & Ostrowski, M., 1998, Phys. Rev. Lett., 80, 3911
 Blandford, R. D., Ostriker, J. P., 1978, ApJ, 221, L29
 Blandford, R. D., Königl, A., 1979, ApJ, 232, 34
 Crider, A., Liang, E. P., Preece, R. D., et al., 1999, ApJ, 519, 206
 De Pasquale, M., Piro, L., Gendre, B., et al., 2005, astro-ph/0507708
 Donato, D., Sambruna, R. M., & Gliozzi, M., 2005, A&A, 433, 1163

Ford, L. A., Band, D. L., Matteson, J. L., et al., 1995, *ApJ*, 439, 307
Gotthelf, E. V., 2003, *ApJ*, 591, 361
Heddal, C. B., Haugbølle, T., Frederiksen, J. T., & Nordlund, Å., 2004, *ApJ*, 617, L107
Kirk, J. G., Guthmann, A. W., Gallant, Y. A., Achterberg, A., 2000, *ApJ*, 542, 235
Kumar, P., & Panaiteescu, A., 2000, *ApJ*, 541, L9
Lemoine, M., & Pelletier, G., 2003, *ApJ*, 589, L73
Lyutikov, M., & Blandford, R., 2003, *astro-ph/0312347*
McMahon, E., Kumar, P., & Piran, T., 2006, *MNRAS*, 366, 575
Niemiec & Ostrowski, 2004, *ApJ*, 610, 851
O'Brien, P. T., Willingale, R., Osborne, J., et al. 2006, *astro-ph/0601125*
Ostrowski, M., & Bednarz, J., 2002, *A&A*, 394, 1141
Panaiteescu, A., & Mészáros, P., 2000, *ApJ*, 544, L17
Piran, T., 2004, *Reviews of Modern Physics*, 76, 1143
Preece, R. D., Pendleton, G. N., et al. 1998, *ApJ*, 496, 849
Preece, R. D., Briggs, M. S., Mallozzi, R. S., et al. 2000, *ApJS*, 126, 19
Preece, R. D., Briggs, M. S., Giblin, T. W., et al., 2002, *ApJ*, 581, 1248
Sikora, M., Begelman, M. C., Rees, M. J., 1994, *ApJ*, 421, 153

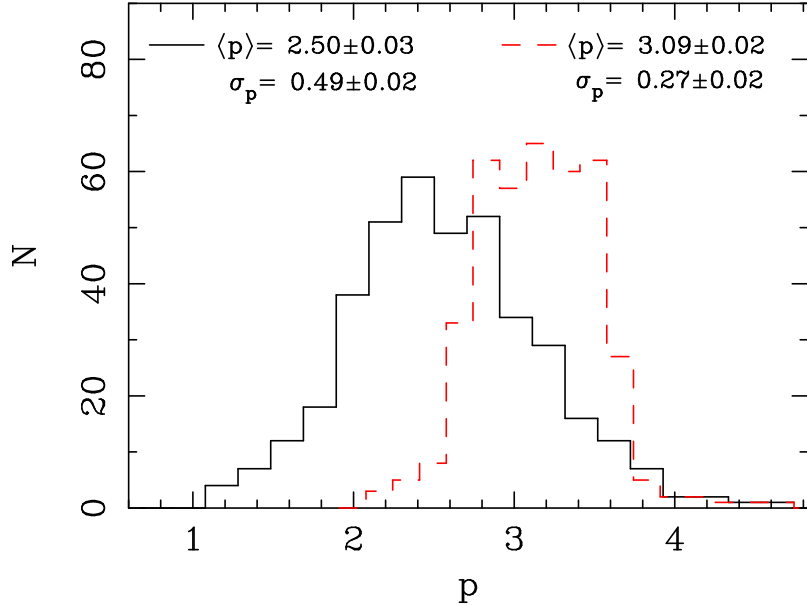


Figure 1. Distributions of p for a sample of 394 GRB spectra with $100 < E_{peak} < 200$ keV. *Solid line*: using the relation $p = -2\beta - 2$. *Dashed line*: after narrowing the distribution by using the relation of either $p = -2\beta - 2$ or $p = -2\beta - 1$.

Spectra samples	100 < E_{peak} < 200 keV		200 < E_{peak} < 300 keV	
	Non-evolving	Evolving	Non-evolving	Evolving
$\langle p \rangle$	2.86 ± 0.06	2.38 ± 0.03	2.50 ± 0.07	2.14 ± 0.03
$\sigma(p)$	0.44 ± 0.04	0.47 ± 0.03	0.58 ± 0.06	0.42 ± 0.03

Table 1. Parameters of parent distribution of p for BATSE GRB spectra samples with E_{peak} -evolution ($\Delta E_{peak} > 15\% E_{peak}$) and without E_{peak} -evolution ($\Delta E_{peak} < 15\% E_{peak}$), where ΔE_{peak} is the E_{peak} difference between any two *adjacent-in-time* spectra. All spectra are assumed in “fast cooling” regime.

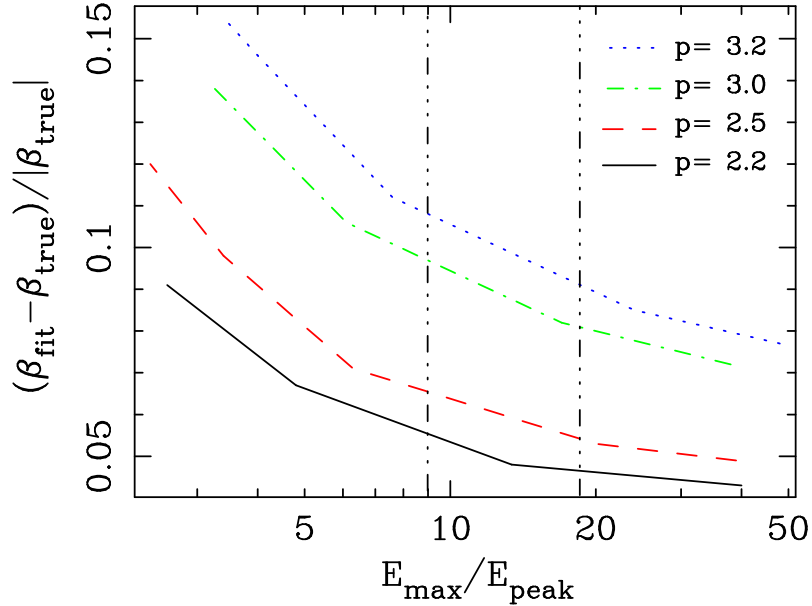


Figure 2. The discrepancy between the fitted value and the ‘true’ value of β , as a function of the higher end of the fitting energy range for the synchrotron spectra fitted by the ‘Band’ function. Two vertical lines mark the range of E_{\max}/E_{peak} corresponding to the E_{peak} range of the sample in Fig. 1. The errors of the spectrum data are assumed to be proportional to square root of photon counts: $\sigma(N(\nu)) \propto \sqrt{N(\nu)}$.

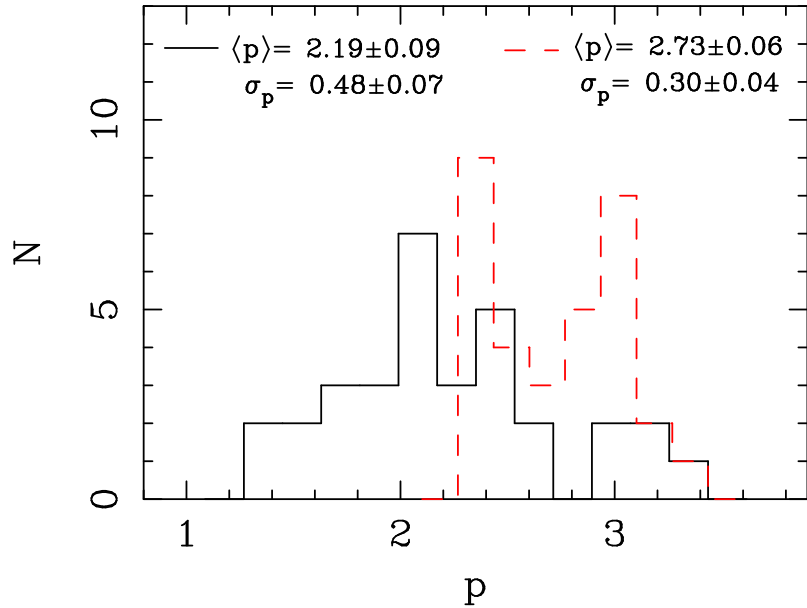


Figure 3. The distribution of p determined from 32 time-integrated GRB spectra. *Solid line*: p is inferred from the high-energy power-law index β by the relation $p = -2\beta - 2$. *Dashed line*: the narrowest distribution of p using the relation either $p = -2\beta - 2$ or $p = -2\beta - 1$. β is taken from the ‘Band’-function fit by Band et al. (1993) to the time-integrated spectrum for each burst.

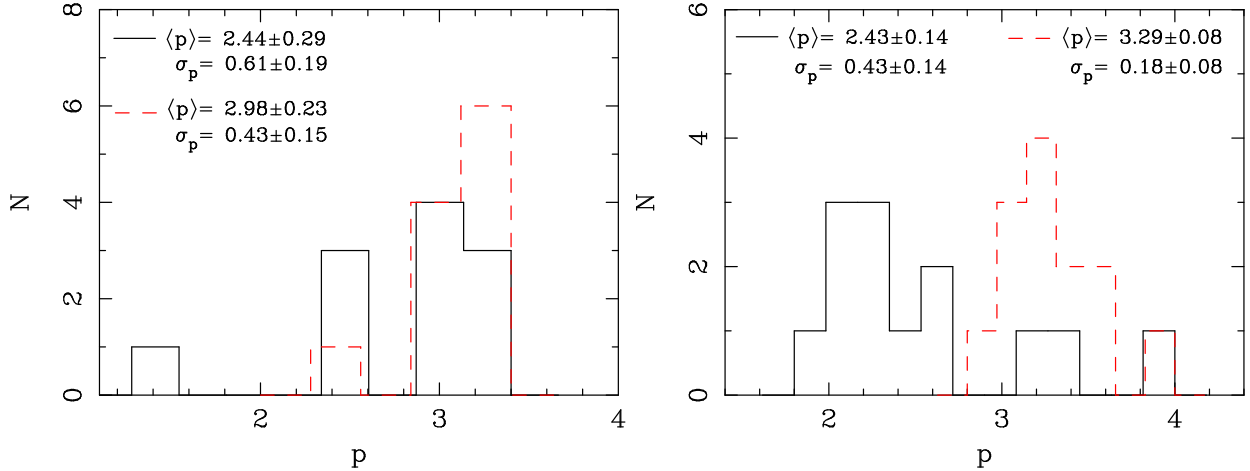


Figure 4. *Left:* The distributions of p for 11 GRBs observed by BeppoSAX (Amati et al. 2002); *Right:* The distributions of p for 13 X-ray flashes, X-ray-rich GRBs and GRBs observed by HETE-2 (Sakamoto et al. 2005). *Solid lines:* p is inferred from the higher-energy photon index β by the relation $p = -2\beta - 2$. *Dashed lines:* the narrowest distributions of p using the relation either $p = -2\beta - 2$ or $p = -2\beta - 1$.

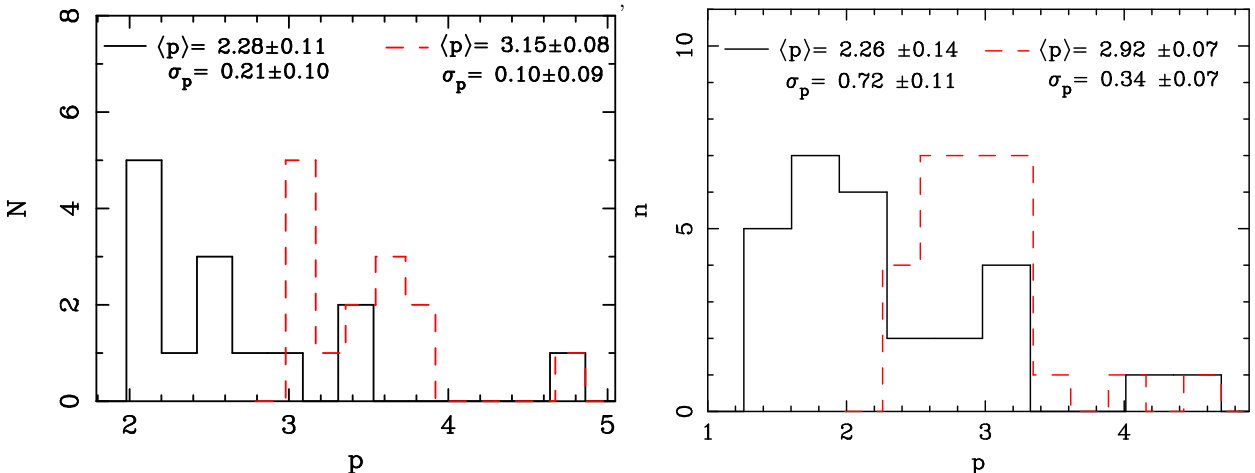


Figure 5. The distributions of p for GRB X-ray afterglows. *Left:* 14 afterglows are observed by BeppoSAX, taken from De Pasquale (2005). *Right:* 28 afterglows are observed by Swift, taken from O'Brien et al. (2006). *Solid lines:* p is inferred from the photon index β by the relation $p = -2\beta - 2$. *Dashed lines:* the narrowest distribution of p using the relation either $p = -2\beta - 2$ or $p = -2\beta - 1$.

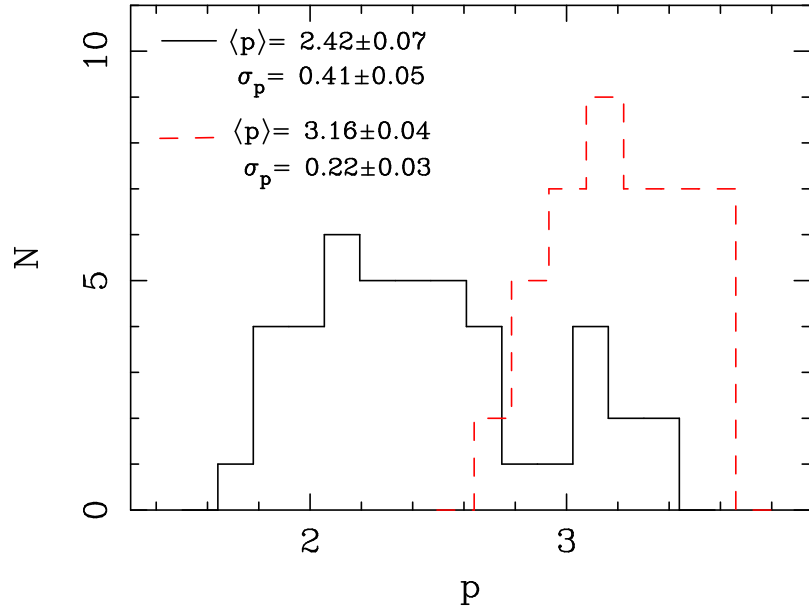


Figure 6. The distribution of p for 44 X-ray spectra of 33 blazars. *Solid* line: p is inferred from the photon index β by the relation $p = -2\beta - 2$. *Dashed* line: the narrowest distribution of p using the relation either $p = -2\beta - 2$ or $p = -2\beta - 1$. β is taken from the catalog compiled by Donato et al. (2005).